

GaPc-Cl films of ca. 1.0 μm thickness were vacuum deposited on optically transparent platinum substrates and placed in contact with the same aqueous ferri/ferrocyanide redox couple. Upon illumination (Figure 1b), the entire current-voltage curve is displaced *positively* from the true $E^{\circ'}$ to the E_{FB} of the Pt/GaPc-Cl system, by an amount $V_{\text{oc}}(2) \approx +0.30$ V. The difference in the E_{FB} of the Au/GaPc-Cl and Pt/GaPc-Cl system is due to the difference in the *effective* work functions of the two metal substrates.⁸ Tabulated values of the work function for clean Pt surfaces range from 5.65 to 5.75 eV (below the energy of an electron in vacuum) while those for Au are typically near 4.8 eV.⁹ The predicted work function difference of 0.8 V or greater is not quite realized in the photoelectrochemical cells where $|V_{\text{oc}}(1)| + |V_{\text{oc}}(2)| = V_{\text{oc}}(3) \leq 0.65$ V. The first molecular layers of GaPc-Cl deposited from vacuum may be expected to lower the effective work function to the observed value as would other hydrocarbon constituents of the Pt-MPOTE surface.⁹

The Pt/GaPc-Cl films fabricated so far tend to have a higher porosity to solution reactants compared to the typical Au/GaPc-Cl films (as evidenced by the larger dark currents observed), which leads to some lowering of photopotential because of short-circuiting of the photoelectrochemical process at the exposed metal sites.¹⁰ In photoelectrochemical cells using unstirred solutions, we have found that the dark current process is inhibited relative to that at photoactive sites. Reasonable photopotentials and photocurrents are still observed on films where the dark currents are up to 50% of those seen on the bare metals.¹⁰

Figure 2 shows a schematic of the Au/GaPc-Cl/ferri,ferrocyanide/GaPc-Cl/Pt photoelectrochemical cell as we hypothesize it exists prior to contact of any of the phases. This schematic is based upon our recent electrochemical and photoelectrochemical studies of band edges and work functions, vs. the ferri,ferrocyanide redox couple solution potential.^{2,3} The relative band energies are those that are expected under strong illumination conditions, i.e., with the Au/Pc and Pt/Pc systems driven to their flatband condition. The expected open-circuit potentials for Au/Pc vs. R/Ox and Pt/Pc vs. R/Ox are shown as $V_{\text{oc}}(1)$ and $V_{\text{oc}}(2)$, respectively. We have found that the $E_{\text{F}}(\text{GaPc-Cl})$ can lie ca. 0.1 V positive of the $E_{\text{F}}(\text{Au})$ and 0.3 V or more positive of the $E^{\circ'}$ of $\text{Fe}(\text{CN})_6^{3-}/\text{Fe}(\text{CN})_6^{4-}$.³ Upon contact of these phases in the dark, the Pc layer becomes charge depleted at both the Au/Pc and Pc/R,Ox interface. The *net* potential gradient in the Au/GaPc-Cl films at equilibrium, however, is such that photogenerated holes under strong illumination are still driven to the Pc/R,Ox interface. For the Pt/GaPc-Cl system, photogenerated electrons are driven to the Pc/R,Ox interface by the *net* electric field gradient within that film.

The photopotential was observed at various load currents for a Au/GaPc-Cl/ferri,ferrocyanide/GaPc-Cl/Pt electrochemical cell under ca. 100 mW/cm² polychromatic illumination (filtered to 470-900 nm) of *both* the photoelectrodes, in contact with 10⁻³ M amounts of $\text{Fe}(\text{CN})_6^{4-}$ and $\text{Fe}(\text{CN})_6^{3-}$. The open-circuit photovoltage was ca. +0.55 V, the short-circuit current 0.1 mA/cm², and the fill factor 0.55 for the most optimized cells. Using maximal power values, the power conversion efficiency was determined to be 0.03-0.05%. Since the cell was not optimized to minimize light losses, this efficiency may be low by a factor of 2-3. Cells with 10 mM redox electrolyte concentrations yielded higher short-circuit currents (by a factor of 3-4) but with lower fill factors (near 0.3). At higher electrolyte concentrations the *i/V* curves were nearly linear with a slope dictated by film resistance, thus leading to the poorer fill factors. The Pt/GaPc-Cl

films tend to exhibit lower photoconductivities than the counterpart Au/GaPc-Cl films. Even when the electrodes are produced simultaneously, such that the Pc films appear to be identical as determined by electron microscopy and spectroscopic assay,¹² the films formed on the Pt-MPOTE are more resistive and less stable than the films formed on the Au-MPOTE.

These cells demonstrate a *thin-film* photovoltaic system where the driving force for the photoelectrochemical response is provided solely by the work function difference between the two metals. The Pc films act as the charge-separating medium and the electrolyte acts as the third contacting phase, less likely to cause short-circuiting of the photoresponse than a metal contact.⁵ The resulting cell gives a photopotential response ca. 20% of the theoretical maximum dictated by the sum of the apparent bandgaps (ca. 3.0 eV) of the two GaPc-Cl/metal systems.¹¹ This technology may lend itself to additional improvements in performance through miniaturization of both the photoactive surfaces and the electrolyte layer between them.

Acknowledgment. This research was supported by grants from the National Science Foundation, CHE83-17769, and IBM Corp. We also thank Len Raymond of the Microelectronics Laboratory at the University of Arizona for the fabrication of the Pt-MPOTE.

(11) Rieke, P. C. Ph.D. Dissertation, University of Arizona, Tucson, 1984.

(12) Visible transmission spectroscopy of thin films of GaPc-Cl (≤ 500 nm) shows an absorbance band extending from ca. 500 to 850 nm with an absorptivity β of $\geq 5 \times 10^4$ cm⁻¹. Thicker films (1 μm) show similar absorbance spectra when examined by photoacoustic spectroscopy. Assay of GaPc-Cl surface coverage is made by dissolving the film in a small volume of pyridine and quantitating the resultant solution concentration from the absorbance spectrum (see ref 11).

Size and Selectivity in Zeolite Chemistry. A Remarkable Effect of Additive on the Products Produced in the Photolyses of Ketones

Nicholas J. Turro,* Chen-Chih Cheng, and Xue-Gong Lei

Chemistry Department, Columbia University
New York, New York 10027

Edith M. Flanigen

Union Carbide Corporation
Tarrytown Technical Center
Tarrytown, New York 10591
Received January 25, 1985

Photolyses of dibenzyl ketones adsorbed on zeolites have been reported to result in decarbonylation and coupling of the resulting radicals to produce diaryl ethanes as the major products.¹ We report that the products formed in the photolysis of dibenzyl ketones on certain zeolites can be extremely sensitive both to zeolite structure and to simple sorbed additives such as water, benzene, cyclohexane, and hexane.

The zeolites² investigated were NaA, NaX, NaY, and LZ-105. Dibenzyl ketone (DBK) and *p*-methylbenzyl benzyl ketone (*p*-MeDBK) were deposited on the zeolites² from pentane solutions,³

(1) (a) Turro, N. J.; Wan, P. *J. Am. Chem. Soc.* **1985**, *107*, 678. (b) For other publications dealing with photochemistry on zeolites, see: Casal, H. L.; Scaiano, J. C. *Can. J. Chem.* **1984**, *62*, 628. Suib, S. L.; Kostapapas, A. *J. Am. Chem. Soc.* **1984**, *106*, 7705. Baretz, B. H.; Turro, N. J. *J. Photochem.* **1984**, *24*, 201. Turro, N. J.; Wan, P. *Tetrahedron Lett.* **1984**, 3665.

(2) The zeolite samples were Linde Molecular Sieves obtained from the Union Carbide Corp. The zeolites employed were sodium exchanged with concentrated aqueous NaCl and subsequently baked at 550 °C for at least 6 h. A further baking at 550 °C for 1 h was employed just before sample preparation, with care being taken to minimize the time which the sample was exposed to the atmosphere.

(3) In a typical experimental 0.4 mg of ketone in 0.2 mL of pentane was added to a vial containing 40 mg of zeolite soaked in a minimum amount of pentane. The bulk of the solvent was rapidly removed by placing the sample in a warm (50 °C) stream of flowing air. The sample was then placed into a quartz photolysis cell, equipped with a side arm, which allowed vacuum (2×10^{-4} torr) degassing.

(8) (a) Rose, A. *Phys. Status Solidi* **1979**, *56*, 11. (b) Rose, A. "Concepts in Photoconductivity and Allied Problem"; R. E. Krieger Pub. Co.; New York, 1978.

(9) (a) Riviere, J. C. In "Solid State Surface Science"; Green, M. Ed.; Marcel Dekker: New York, 1969; Vol. I, pp 179. (b) "CRC Handbook of Chemistry and Physics", 58th ed.; Weast, R. C., Ed.; Cleveland, 1977-78, p E-81.

(10) (a) Rieke, P. C.; Linkous, C. L.; Armstrong, N. R. *J. Phys. Chem.* **1984**, *88*, 1351. (b) Klofta, T. J.; Rieke, P. C.; Linkous, C. L.; Buttner, W. J.; Nanthakumar, A.; Mewborn, T.; Armstrong, N. R. *J. Electrochem. Soc.*, submitted for publication.

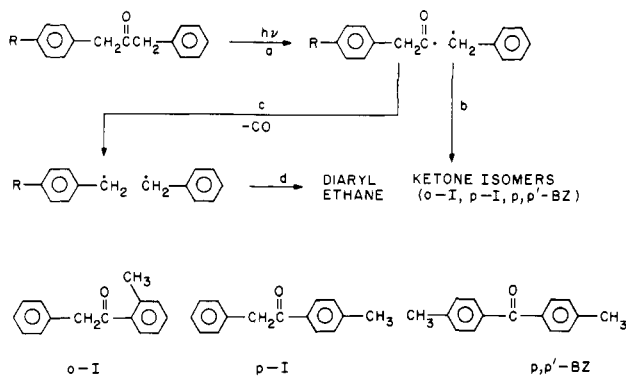


Figure 1. Schematic of the photolysis of dibenzyl ketone (DBK, R = H) and *p*-methylbenzyl benzyl ketone (*p*-MeDBK). Step (a) consists of absorption, formation of S_1 , intersystem crossing to T_1 , and cleavage to produce a primary geminate radical pair. The latter may either undergo coupling to produce ketone isomers (b) or loose carbon monoxide (c) to produce a secondary geminate radical pair. The latter may either undergo cage coupling (d) or diffusional separation to form random free radicals which eventually couple.

degassed under vacuum and photolyzed,⁴ extracted into benzene, and analyzed by VPC.⁵ Experiments were run without the addition of any additive after the vacuum removal of pentane and with the addition of controlled amounts of water, benzene, cyclohexane, and hexane which was admitted as vapor to the zeolite samples.⁶

The entrance pore opening of NaA (ca. 4 Å) is too small to allow entrance of DBK or *p*-MeDBK to the internal voids of this zeolite.⁷ The observed results are completely analogous to those observed in homogeneous solution⁸ (diaryl ethanes only, cage effect, 0%) and are unaltered for NaA systems containing additives. These results contrast strongly with those found for photolysis of DBK or *p*-MeDBK on NaX, NaY, and LZ-105. The pore openings of NaX and NaY (ca. 8-Å diameter) are large⁷ enough to allow ready access to the internal zeolite voids by the ketones (minimum kinetic diameter ca. 7 Å) investigated. For thoroughly dehydrated NaX and NaY, the yields of DPE from DBK are 60% and 85%, respectively, and the cage effects for *p*-MeDBK are 18% and 19%, respectively. The remaining mass balance is due to isomers (Figure 1) of DBK (*p*-I and *o*-I) which are formed in addition to DPE on both NaX and NaY. *p*-I is the major isomer in both cases. *The product distributions formed on NaX and NaY were found to be strikingly sensitive to additives admitted from the vapor phase.*⁶ In the case of NaX, the yield of DPE plunges from 60% to 6% when benzene vapor is added to the system. For NaY, the yield of DPE plunges less dramatically from 85% to 37%. Simultaneously, *isomers of DBK (Figure 1) become the major products of photolysis.* For NaX, *o*-I is the major isomer (52%), and for NaY, *p,p'*-BZ is the major isomer (33%). The ratio of isomers could also be varied by addition of cyclohexane to the systems. In this case, *o*-I was the major isomer for NaX and *p*-I was the major product for NaY. Addition of *n*-C₆H₁₄ to NaX or NaY had qualitatively the same effect as addition of *c*-C₆H₁₂. However, the yield of isomers of DBK was lower as was the cage effect for *p*-MeDBK. Addition

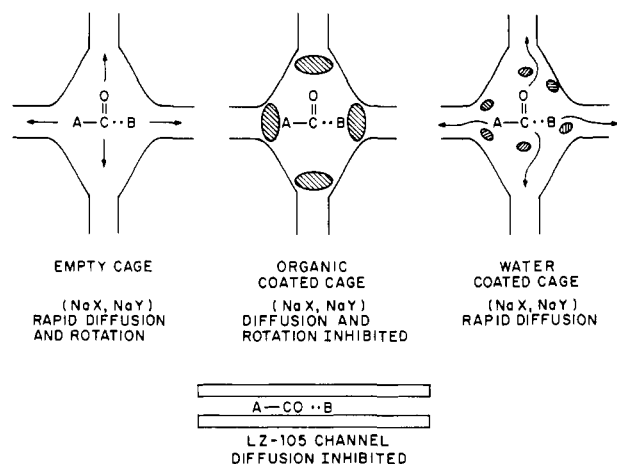


Figure 2. Schematic representation of the situations for primary radical pair: top left, vacuum; top middle, organic additives; top right, water additive.

of H₂O to NaX or NaY produced significantly different results compared to those observed with hydrocarbon additives. Only traces of isomers of DBK were observed, and the cage effect was smaller.

The pore openings⁹ of LZ-105 (ca. 6-Å diameter) are somewhat smaller than those of NaX and NaY but large enough to allow ready absorption of DBK and *p*-MeDBK into the interval cavities.⁷ Photolysis of DBK and *p*-MeDBK on LZ-105 resulted in a large cage effect (90%), and additives from the vapor phase had virtually no effect on the product distribution.

The internal zeolite framework structure of NaX and NaY are very similar,⁷ but NaX is more hydrophilic than NaY and contains more internal cage sodium ions (to balance the charge associated with framework Al atoms). The internal supercages of NaX and NaY are rather large (ca. 13-Å width) so that the radical pairs produced by photolysis of the DBKs can readily separate and diffuse apart. Such freedom of diffusional motion encourages loss of CO from the primary radical pairs and a small cage effect due to the relatively free diffusional activity of the secondary radical pairs which eventually couple to yield diarylethanes (Figure 2).

The additives are postulated to fill up the remaining void space in the supercage cavities and the additive molecules tend to serve as a thin-walled molecular cage within the zeolite cages. The inclusion of organic molecules in the same supercage as a ketone will cause congestion of the available void space and will seriously restrict the diffusional and, less so, rotational motion of the radical pairs produced by photolysis of DBK. As a result, recombinations of the primary radicals are encouraged relative to the situation in the absence of additives, and isomerization becomes competitive or favored relative to diffusional separation and to decarbonylation (Figure 2). The efficiency of cage recombination of decarbonylated radical pairs will also increase. The addition of water molecules causes quite a different result. It would appear that both primary and secondary radical pairs experience greater diffusional freedom in cages filled with water than in cages filled with organic molecules. These conclusions are consistent with NMR investigations of benzene¹⁰ and water¹¹ adsorbed on NaX.

In the case of LZ-105, the dimensions of the internal channels are close to that of the benzyl fragments of the ketones¹ studied. In contrast to the situation for NaX and NaY, diffusion and rotational motions are both inhibited, and only regeneration of DBK and loss of CO would be expected to result from the primary radical pair; ketone isomerization is effectively inhibited. That

(4) The sample was maintained under vacuum and tumbled during photolysis (313 nm) at ambient temperature.

(5) After irradiation the sample was washed with benzene (LZ-105) or with CH₂Cl₂ (NaA, NaX, NaY). The extracted organic material was then concentrated by solvent evaporation and then dissolved in anhydrous ether before analysis.

(6) The additives were introduced by following the procedure described in ref 2, except that prior to photolysis the sample was exposed to the vapor from a reservoir of pure additive liquid located in a side arm of the cell. The total cell was thoroughly degassed via the freeze-thaw technique before the vapor was admitted to the sample.

(7) (a) Derouane, E. G. "Intercalation Chemistry"; Whittingham, M. S., Jacobson, A. J., Eds.; Academic Press: New York, 1982; p 101. (b) Breck, D. W. "Zeolite Molecular Sieves"; Wiley: New York, 1974.

(8) Engel, P. S. *J. Am. Chem. Soc.* **1970**, *92*, 6074. Robbins, W. K.; Eastman, R. H. *Ibid.* **1970**, *92*, 6076.

(9) The internal surface of LZ-105 is typical of zeolites and the ZSM family, i.e., intersecting channels. For a discussion, see: DeRoune, E. G. "Catalysis by Zeolites"; Imelik, B., et al., Eds.; Elsevier: Amsterdam, 1980; p 5.

(10) Parravano, C.; Baldeschwieler, J. D.; Boudart, M. *Science (Washington, D.C.)* **1967**, *155*, 1535.

(11) Ruthven, D. M. "Principles of Adsorption and Adsorption Processes"; Wiley: New York, 1984.

the lack of isomerization is not due simply to rapid diffusional separation of the radical pairs is supported by the generally lower efficiency of photolysis on LZ-105 relative to NaX or NaY and by the high cage efficiency for combination of benzyl radicals. Also consistent with this mechanism is the absence of any significant influence of additives on the course of the photolysis. None of the results appear to require cation-specific effects, although such factors may be involved in determining the differences observed with some of the additives.

The fact that the major products of reaction formed on NaY changes from *p,p'*-BZ for benzene as additive to *p*-I for cyclohexane as additive is remarkable and demonstrates the high sensitivity of radical pair rotational motion anisotropies to the

shape and size of the molecular species employed as a cavity filler. Further confirmation of this conclusion is provided by the observation that the major isomeric product from DBK in "empty" NaX is *p*-I, whereas the major isomeric product when benzene is added is *o*-I. These results attest to the high size and shape selectivity for adsorption of molecules on zeolites.

Acknowledgment. The authors at Columbia thank the National Science Foundation for their generous support of this research. They also thank Professor D. M. Ruthven, University of New Brunswick, Canada, for helpful discussions concerning diffusion and sorption in zeolites.

Registry No. DBK, 102-04-5; *p*-MeDBX, 35730-02-0.

Additions and Corrections

Zoanthamine: A Novel Alkaloid from a Marine Zoanthid [*J. Am. Chem. Soc.* **1984**, *106*, 7983-7984]. C. BHEEMASANKARA RAO,* A. S. R. ANJANEYULU, N. S. SARMA, Y. VENKATESWARLU, RICHARD M. ROSSER, D. JOHN FAULKNER,* MARINE H. M. CHEN, and JON CLARDY*

Page 7983: In the author listing, Anjaneyulu and Venkateswarlu are incorrectly spelled. In the second paragraph, the yield should read ($9 \times 10^{-4}\%$ wet weight).

Treatment of Electrostatic Effects within the Molecular Mechanics Method. [*J. Am. Chem. Soc.* **1983**, *105*, 1716]. LJILJANA DOŠEN-MICOVIĆ, DRAGOSLAV JEREMIC, and NORMAN L. ALLINGER*

Page 1718: Equation 6 should read:

$$\mu_{ix} = \sum_{j=1}^n (B_{3i-2,3j-2}\mu_{jx}^{\circ} + B_{3i-2,3j-1}\mu_{jy}^{\circ} + B_{3i-2,3j}\mu_{jz}^{\circ})$$

$$\mu_{iy} = \sum_{j=1}^n (B_{3i-1,3j-2}\mu_{jx}^{\circ} + B_{3i-1,3j-1}\mu_{jy}^{\circ} + B_{3i-1,3j}\mu_{jz}^{\circ})$$

$$\mu_{iz} = \sum_{j=1}^n (B_{3i,3j-2}\mu_{jx}^{\circ} + B_{3i,3j-1}\mu_{jy}^{\circ} + B_{3i,3j}\mu_{jz}^{\circ})$$

Page 1719: In eq 18 the first row should look as follows:

$$\gamma_{H(C)}\gamma_{C(H)} > \gamma_{C(C)}$$

Page 1720: The caption to Figure 1 should refer to ref 35 not ref 32.

Page 1722: In Table III columns 7, 8, and 9 are mixed up. They should look as follows:

Table III. The IDME Parameter Set

	bond (J-P)		
	...C-Cl	C-Br	C=O
ν_{JP}	0.56	0.54	0.68
$\gamma_{J(P)}$	0.2	0.2	0.2
$\gamma_{J(P)}$	0.4	0.4	0.4
σ_J^0	0.07	0.07	0.07
σ_P^0	0.35	0.30	0.70
LP	3.8 (2.9) ^c	5.3 (3.1) ^c	2.3
TP	1.85 (2.2)	2.7 (3.1)	1.4
VP	1.85 (2.2)	2.7 (3.1)	0.46
CR(J)	0.771	0.771	0.771
CR(P)	0.99	1.14	0.638

The dipole field tensor T_{ij} , which has not been given explicitly in the paper looks as follows:

$$T_{ij} = -\frac{3}{\epsilon r^5} \begin{vmatrix} x^2-(r^2/3) & xy & xz \\ yx & y^2-(r^2/3) & yz \\ zx & zy & z^2-(r^2/3) \end{vmatrix}$$

where r is the distance between dipoles i and j ; x , y , z are the components of the vector from i to j ; and ϵ is the medium dielectric constant, equal 1.5 for the vapor phase in our calculations.